Multiphysics Between Deep Geothermal Water Cycle, Surface Heat Exchanger Cycle and Geothermal Power Plant Cycle

Li Wah Wong[*,1], Guido Blöcher[1], Oliver Kastner[1], Günter Zimmermann[1]
[1]International Centre for Geothermal Research (ICGR GERMANY)
*Helmholtz Centre Potsdam, GFZ German Research Centre For Geosciences, Telegrafenberg, D-14473 Potsdam, Germany, liwah.wong@gfz-potsdam.de

Abstract: This is a multiphysics study in the framework of Groß Schönebeck (GrSk) project in the North German Basin of Germany. Multiphysics (couplings) between four major components i.e. deep geothermal reservoir, boreholes, heat exchangers and geothermal power plant is crucial in order to study lifecycle behavior of each component thereafter a later coupling to study lifecycle and recovery of the overall geothermal system. Study is divided into three main cycles i.e. geothermal water cycle, surface heat exchanger cycle and power plant cycle. Geothermal water cycle is weighted in the first place and began with a standalone 3D deep geothermal reservoir model which is composed of fractures, wells and fault zones. Subsurface fluid flow is coupled to heat transfer in porous medium. This cycle is solved for a period of 30 years and the result will be linked via an interface to surface heat exchanger cycle, as the advanced coupling process, before another further coupling with the geothermal power plant cycle.

Keywords: hydraulic induced fractures, permeable internal fault zones, Darcy's, fluid heat transfer

1. Introduction

The local geology of North German Basin of Germany is representative for many parts of Western and Central Europe therein represents an important pilot for geothermal technology development in Europe. GFZ German Research Centre For Geosciences reveals that a conversion of deep geothermal energy into electricity requires a temperature of about 150°C and a minimum flow rate of 50m^3/h. Multiphysics (couplings) between three major cycles of a deep geothermal system i.e. (subsurface) geothermal water cycle, surface heat exchanger cycle and power plant cycle is ultimate to study the optimization of net electricity provision and the recovery of the overall geothermal system. Subsurface geothermal cycle is illustrated as a coupled 3D deep geothermal reservoir model, at which later is coupled to the surface heat exchanger cycle via an interface, following by a further coupling with the geothermal power plant cycle. In order to study the hydrothermal (HT) process and according to Blöcher *et al.* (2010), 3D deep geothermal reservoir model consists of an injection well E GrSk 3/90, a deviated production well Gt GrSk 4/05 (18° - 48°), a hydraulically induced multifracture (two gel proppant fractures, two water fractures) along the injection well, three likewise fractures (one water fracture, two gel proppant fractures) along the production well and three internal natural fault zones (f21n, f28, f29), between the depth -3815m to -4236m below sea level in the Lower Permian of the North German Basin. With the simplification of a constant injection temperature of 70°C, dependant variables, pressure and temperature, are solved at a time, for a period of 30 years.

2. Governing Equations

2.1 Darcy's Law

Permeability model is selected to specify the capacity of the reservoir porous material to transmit flow. With the assumption of laminar flow between parallel plates, permeability, k, [m^2] of the three major natural fault zones, f21n, f28 and f29, is related to aperture, d_f, [m], of the hydraulically induced fractures at which $d_f = a^2/12$ and that laminar flow obeys Darcy's Law.

$$u = -\frac{k}{\mu}(\nabla p + \rho g \nabla D) \text{ [m/s]} \quad (1)$$

Hydraulic conductivity, K, [m/s], is selected to define a combination of fluid permeability, p, [m^2] and dynamic viscosity, μ, [Pa·s] of each geological layer or the reservoir,

$$u = -\frac{K}{\rho g}(\nabla p + \rho g \nabla D) \text{ [m/s]} \quad (2)$$

2.2 Heat Transfer in Fluid

By defining a heat equation for heat transfer in fluid, five important reservoir material properties are density, ρ, [kg/m^3], fluid heat capacity at constant pressure, C_p, [J/(kg*K)], which describes the amount of heat energy required to produce a unit temperature change in a unit mass, fluid thermal conductivity, k, [W/(m*K)], which is a scalar or a tensor if the thermal conductivity is anisotropic, fluid velocity field, u, [m/s], which takes the value of Darcy's velocity as per definition in 2.1, and heat source (or sink), Q, [W/m^2]. The first four are defined for each geological layer respectively and the fifth is defined for the bottom of the reservoir, 72E-03W/m^2 in a stationary state.

$$\rho C_p \frac{dT}{dt} + \rho C_p \mathrm{u} \cdot \nabla T = \nabla \cdot (k \nabla T) + Q \qquad (3)$$

In a stationary state, temperature does not change with time therein the first term disappears.

$$\rho C_p \mathrm{u} \cdot \nabla T = \nabla \cdot (k \nabla T) + Q \qquad (4)$$

3. Use of COMSOL Multiphysics

Mathematical model based on a steady state is a boundary value problem, at which field variables i.e. hydraulic head is specified along the reservoir boundaries, referred to as boundary conditions which are solved for values of the field variables at any point within the reservoir. Both boundary conditions and computed values of the field variables do not change with time. Maximum and minimum values of the field variables thereafter occur on the reservoir boundaries.

On the other hand, a mathematical model based on a time dependant state is an initial value problem. Values of the field variables are specified at all points within the reservoir at a particular initial time t_0 and are referred as initial conditions and can be solved at any point at time $t>t_0$.

3.1 Finite Element Method

Numerical method chosen in this study is a finite element method, for the sake of numerical solutions for the case of anisotropic and heterogeneous reservoir material, fluid, hydraulic and thermal properties. Significantly, the deviated production well Gt GrSk 4/05 which is inclined at 18° from the top of the reservoir (-3815m) and increases progressively to 48° at -4236m, can be easily incorporated into the numerical model. Reservoir domain is discretized, in other words, replaced by a collection of nodes (nodal points) and elements referred to as finite element mesh. Reservoir material, fluid, hydraulic and thermal properties are specified for each element, which are constant within the element itself but may vary from one element to the next in principle.

3.2 Darcy's Law Physics Interface

The approximate solution from Darcy's Law is expected to be continuous along the boundary between adjacent elements, in other words, is continuous from one element to the next throughout the domain.

$$\frac{\partial}{\partial \mathrm{t}}(\rho\varepsilon) + \nabla \cdot (\rho \mathrm{u}) = Q_m \qquad (5)$$

A homogenization of the porous and fluid media into a single medium is the alternative approach and Darcy's Law is combined with the continuity equation (5) and equation of state for the pore fluid, which complete a porous media flow for which the pressure gradient, which takes the gravity effects into account, is the major driving force.

$$\frac{\partial}{\partial \mathrm{t}}(\rho\varepsilon) + \nabla \cdot \rho[-\frac{k}{\mu}(\nabla p + \rho \mathrm{g} \nabla \mathrm{D})] = Q_m \qquad (6)$$

Expanding the time derivative term,

$$\frac{\partial}{\partial \mathrm{t}}(\rho\varepsilon) = \varepsilon \frac{\partial \rho}{\partial \mathrm{t}} + \rho \frac{\partial \varepsilon}{\partial \mathrm{t}} \qquad (7)$$

Defining porosity, ε, [1], and density, ρ, [kg/m^3], as functions of pressure, and applying the chain rule,

$$\varepsilon \frac{\partial \rho}{\partial \mathrm{t}} + \rho \frac{\partial \varepsilon}{\partial \mathrm{t}} = \varepsilon \frac{\partial \rho}{\partial \mathrm{p}} \frac{\partial \mathrm{p}}{\partial \mathrm{t}} + \rho \frac{\partial \varepsilon}{\partial \mathrm{p}} \frac{\partial \mathrm{p}}{\partial \mathrm{t}} \qquad (8)$$

Inserting the definition of fluid compressibility to the right hand side of the equation above,

$$X_f = \left(\frac{1}{\rho}\right)\left(\frac{\partial \rho}{\partial \mathrm{p}}\right) \qquad (9)$$

Rearranging to arrive at,

$$\frac{\partial(\rho\varepsilon)}{\partial \mathrm{t}} = \rho\left(\varepsilon X_f + \frac{\partial \varepsilon}{\partial \mathrm{p}}\right)\frac{\partial \mathrm{p}}{\partial \mathrm{t}} = \rho \mathrm{S}\frac{\partial \mathrm{p}}{\partial \mathrm{t}} \quad (10)$$

The final governing equation includes a storage coefficient, S, [1/Pa], which represents a weighted compressibility of both bulk reservoir material and pore fluid, 1.0E-10/Pa is defined throughout the study.

$$\rho \mathrm{S}\frac{\partial \mathrm{p}}{\partial \mathrm{t}} + \nabla \cdot \rho[-\frac{k}{\mu}(\nabla \mathrm{p} + \rho \mathrm{g}\nabla \mathrm{D})] = Q_m \quad (11)$$

3.3 Heat Transfer in Fluid Physics Interface

Besides defining heat transfer in fluid, heat transfer in porous media is also defined. When it comes to heat conduction, based on the characteristics of each geological layer, thermal conductivity, λ, [W/m*K], describes the relationship between the heat flux factor q and the temperature gradient, ∇T, [K],as in q = - λ ∇T, which is Fourier's law of heat conduction.

When it comes to thermodynamics, based on the characteristics of each geological layer, specific heat capacity, $C_{\mathrm{p,p}}$, [J/(kg*K)], describes the amount of heat energy required to produce a unit temperature change in a unit mass of the reservoir solid material. Density, ρ_{p}, [kg/m^3], and ratio of specific heat, γ [1], of bulk reservoir material are defined respectively. γ of bulk reservoir material is defined as 1 throughout the study.

$$(-\lambda \nabla T) = 0 \quad (12)$$

Equation (12) is a boundary condition of no heat flux across, representing that the reservoir domain is well insulated.

Volume fraction of reservoir solid material, θ_{p}, [1] takes the value of θ_{p} = 1-ε, with different λ, [W/m*K] of each geological layer, heat transfer in reservoir solid material in a stationary state from equation (4),

$$\rho C_{\mathrm{p}} \mathrm{u} \cdot \nabla T = \nabla \cdot (\lambda \nabla T) + Q \quad (13)$$
$$\lambda = \lambda_{\mathrm{eq}} \quad (14)$$
$$\lambda_{\mathrm{eq}} = \theta_{\mathrm{p}}\lambda + (1 - \theta_{\mathrm{p}})\lambda \quad (15)$$

Heat transfer in reservoir solid material in a time dependent state from equation (3),

$$\rho C_{\mathrm{p}} \frac{dT}{dt} + \rho C_{\mathrm{p}} \mathrm{u} \cdot \nabla T = \nabla \cdot (\lambda \nabla T) + Q \quad (16)$$
$$\lambda = \lambda_{\mathrm{eq}} \quad (17)$$
$$\lambda_{\mathrm{eq}} = \theta_{\mathrm{p}}\lambda + (1 - \theta_{\mathrm{p}})\lambda \quad (18)$$
$$\rho C_{\mathrm{p}} = \left(\rho C_{\mathrm{p}}\right)_{\mathrm{eq}} \quad (19)$$
$$\left(\rho C_{\mathrm{p}}\right)_{\mathrm{eq}} = \theta_{\mathrm{p}}\rho_{\mathrm{p}} C_{p,\mathrm{p}} + (1 - \theta_{\mathrm{p}})\rho C_{\mathrm{p}} \quad (20)$$

To calculate the stationary state, a constant temperature of 410.5K is set as boundary condition for the top of reservoir along with a surface heat flow of 72E-03W/m^2 at the bottom of the reservoir as per Norden *et al*. (2008), $(-\lambda \nabla T) = q_0$, q_0 = 72E-03W/m^2, indicating a terrestrial heat flux.

Resulted temperature solution from a stationary state is implemented as initial temperature, T_0, in terms of an interpolated function, *int*, of depth, for a subsequent time dependant state with a *m* number of nodes in the mesh,

$$\sum_{i=1}^{m} int\,(x, y, z)T_0 \quad (21)$$

An injection temperature, $T = T_{\mathrm{inj}}$ = 343K is added to the injection well E GrSk 3/90.

4. Numerical Model

This study is carried out on COMSOL Multiphysics 4.3 platform, Subsurface Flow module and Heat Transfer module are used to couple subsurface fluid flow and heat transfer in porous medium, thereafter Darcy's Law is coupled to advective heat flux.

In the 3D deep geothermal reservoir model, all four hydraulically induced fractures are integrated as 2D extruded faces into geological units which are represented as elements for 3D geometries. Internal fault zones (f21n, f28, f29) are integrated as 2D extruded faces as well. Injection well E GrSk 3/90 and deviated production well Gt GrSk 4/05 are integrated as 1D edges within fractures and fault zones. 3D geometries are a group of 3D solid blocks with a total width of 2650m and length of 2750m, and different heights representing the six significant geological layers of the reservoir respectively.

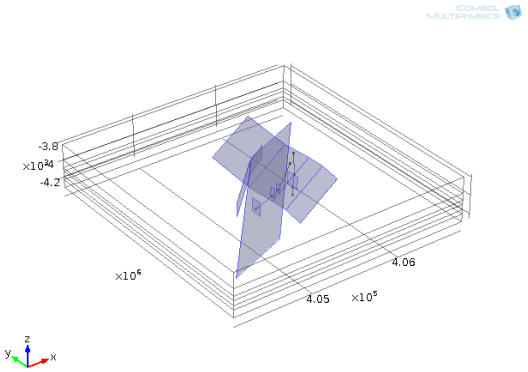

Figure 1. 1D edges (Bézier Polygon) and 2D faces (workplane-extruded Bézier Polygon) within a 3D solid domain

Figure 2 shows that finite element mesh is performed in the way that 2D geometries are discretized into triangular mesh elements and 3D geometries into tetrahedral mesh elements. All edges are discretized into edge elements whereas isolated geometry vertices are discritized into vertex elements. Predefined fine mesh size is applied and meshes grow outward from narrow regions i.e. around internal fault zones and hydraulically induced fractures.

Within Darcy's Law physics interface, a fracture flow interface is coupled to represent not only hydraulically induced fractures with particular thickness, d_f, [m], porosity, ϵ_p, [1], and hydraulic conductivity, K, [m/s] or permeability, k, [m^2],

$$d_f \frac{\partial}{\partial t}(\rho \epsilon_p) + \nabla_T \cdot (d_f \rho u) = d_f Q_m \quad (22)$$

$$u = -\frac{K_f}{\mu}(\nabla_T p + \rho g \nabla D) \quad (23)$$

A production rate of 75m^3/h from GrSk project is expected. An inward mass flux, -n = ρu = N_0 = 20.83kg/s is defined at E GrSk 3/90, and three distinctive outward mass flux, N_0 = -20.83kg/s*0.25, N_0 = 20.83kg/s*0.40 and N_0 = -20.83kg/s*0.35, are defined at the three fractures at Gt GrSk 4/05 respectively. Natural gravity effect, which is a function of fluid density, ρ = 0.0003 [kg/m^3], acceleration of gravity, g_const = 9.80665[m/s^2], and depth, z, [m] takes place throughout the study.

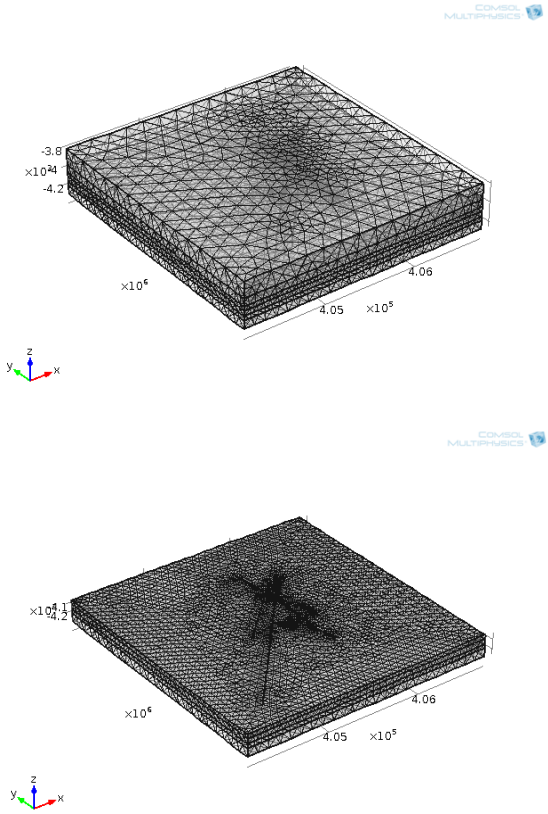

Figure 2. Finite element mesh consisted of triangular, tetrahedral, edge and vertex mesh elements; top: complete meshed model, bottom: internal view

A non faulted 3D deep geothermal reservoir model is simulated as a reference model. To study the effect of internal fault zones on fluid flow and heat transfer in fluid in porous medium, we compared the latter results to the reference model. This study also reveals the effect of the variations of permeability and aperture of internal fault zones on production temperature as well as production index.

5. Results

According to Blöcher *et al*. (2010), field data from Groß Schönebeck project reveals that the aperture, d_f, [m], of hydraulically induced fractures is 2.28E-04m respectively. Assumption is made that internal fault zones possess the same d_f as well as the same K_f and study shows that internal fault zones bring significant effect in reducing temperature drawdown at the

production well Gt GrSk 4/05, along with a constant injection temperature of 70°C for a total period of 30 years. A non fault deep geothermal reservoir encounters a drawdown in production temperature of 27.54°C after 30 years whereas in the case of a faulted deep geothermal reservoir, the temperature drawdown after 30 years of operation is 23.50°C. In the latter case, the production temperature drops from 148.77°C to 125.27°C.

Study is enhanced with a variation in the d_f of internal fault zones and it shows that production temperature drawdown is reduced with an increment in the d_f.

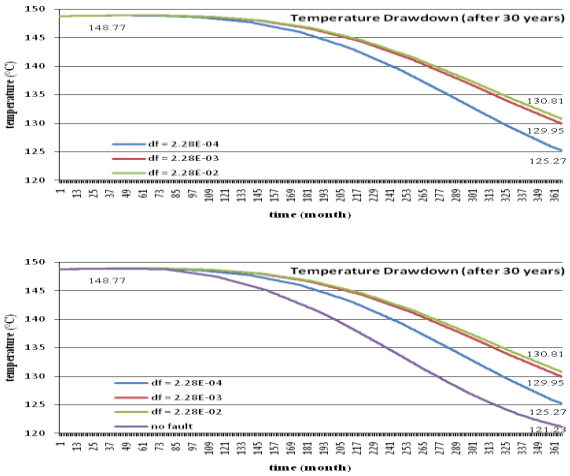

Figure 3. Production temperature drawdown is reduced with the existence of faults and with increment in the d_f; top: comparison of temperature drawdown in different cases of d_f, bottom: comparison of temperature drawdown in a non fault system and a faulted system

Further study is carried out with a variation in the K_f of internal fault zones with d_f = 2.28E-04m, and it shows that temperature drawdown increases with the decrease in K_f. When it is approaching the highest K_f of the reservoir solid material, K_f = 7.90E-15m^2, temperature drawdown stays constant gradually at 31.05°C, as per shown in figure 4.

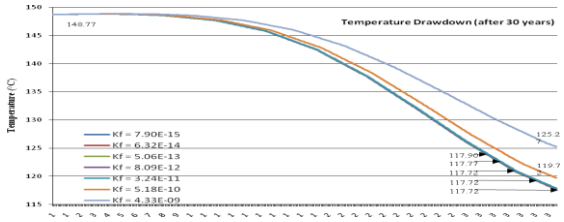

Figure 4. Production temperature drawdown increases with the decrease in permeability of internal fault zones. It stays constant gradually towards K_f = 7.90E-15m^2

Elbe Base Sandstone layer of the North German Basin possesses the highest permeability 7.90E-15m^2 and is the most preferable rock for matrix infiltration, meanwhile with the high hydraulic conductivity of both hydraulically induced fractures and high permeability of the Elbe Base Sandstone layer, figure 5 shows that cold water front (70°C) from the injection well E GrSk 3/90 propagates and reaches the second gel-proppant fracture along the production well Gt GrSk 4/05 after 30 years.

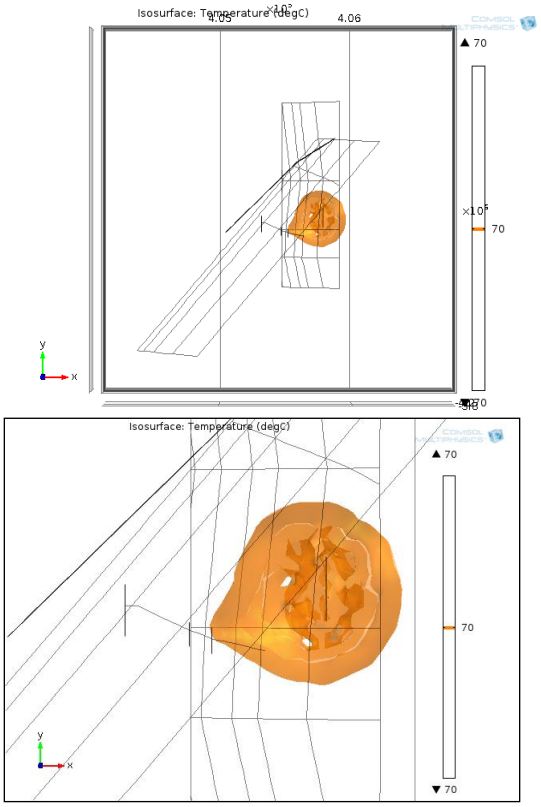

Figure 5. After 30 years, cold water front (70°C) reaches production well causing a significant drop of production temperature to 125.27°C; top: top view of the reservoir, bottom: close up of cold water front reaching production well

With an expected production rate of 75m^3/h from GrSk project, a production index of 6.00 m^3/(h*MPa) is observed throughout 30 years, under the condition of d_f = 2.28E-04m and K_f = 4.33E-09m^2.

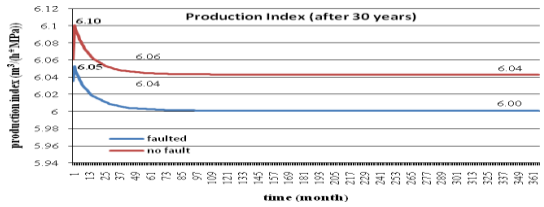

Figure 6. Comparison of production index in a non fault system and a faulted system

6. Conclusion

In an enhanced geothermal system (EGS) like Groß Schönebeck, four major components in the deep geothermal water cycle are hydraulically induced fractures, natural internal fault zones, wells (injection well, production well) and geological units. All of them ought to be combined to perform a well rounded and sophisticated study of the hydrothermal process during the geothermal power production. Previously, deviated geometries such as the production well and dipping geometries such as natural internal fault zones are not supported by any other software platforms. Using Feflow for instance according to Blöcher *et al*. (2010), deviated production well is represented as interlinked 1D vertical elements at which short circuits exist at the three fractures along the production well. Natural internal faults are never implemented so far. COMSOL Multiphysics allows the implementation of deviated production well Gt GrSk 4/05 in 1D such as Bézier curve, 2D such as parametric surface or 3D such as cylinder. The implementation of internal fault zones is performed through linear, cubic or quadratic solid or curve segment extrusion from workplanes. Since natural internal fault zone is successfully implemented, this study weighted the effect of variations of permeability and aperture of internal fault zones on production temperature as well as production index in the first place. Both production temperature and index are calculated by the weighted average of the points between the production well Gt GrSk 4/05 and the three hydraulically induced fractures along, in the ratio of 25%:40%:35%, in the order of water fracture, first gel-proppant fracture and second gel-proppant fracture.

Other feasible variables for sensitivity analysis are fluid density and viscosity, fluid thermal conductivity and capacity, solid thermal conductivity and capacity, permeability, porosity and geological surface heat flow within the framework of Groß Schönebeck (GrSk) project.

7. Outlook

COMSOL Multiphysics 4.3 allows the import of mesh generated by other meshing software (Cacace *et al*. (2012)).

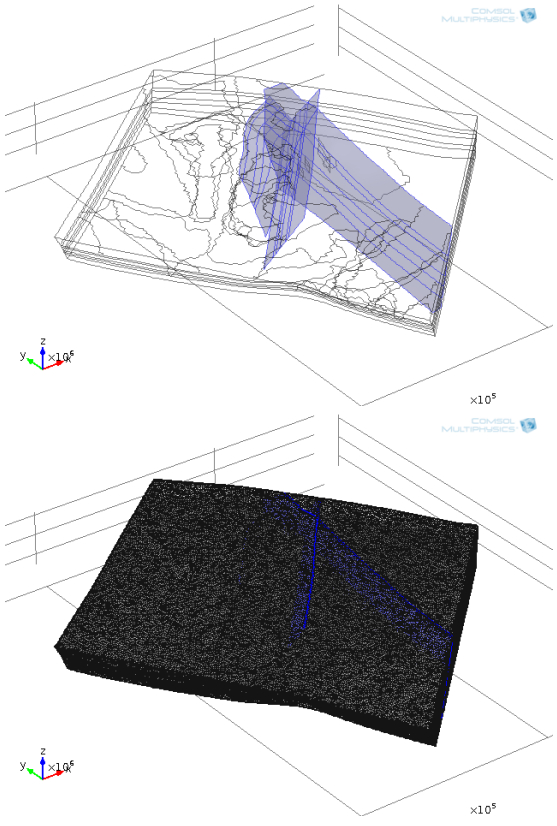

Figure 7. Import of external mesh developed with MeshIT into COMSOL Multiphysics in .mphtxt format

The geothermal water cycle in this study is solved for a period of 30 years and is due to be linked via an interface to surface heat exchanger cycle, as well as feasible advanced coupling processes using other modules, structural mechanics module for instance, before another further coupling with the geothermal power plant cycle.

8. References

1. Holzbecher E., Wong L.W., Litz M.-S., Modelling Flow through Fractures in Porous Media, *European COMSOL Conference*, Paris (2010)
2. Blöcher G., Zimmermann G., Moeck I., Brandt W., Hassanzadegan A., Magri F., 3D numerical modeling of hydrothermal processes during the lifetime of a deep geothermal reservoir, *Geofluids*, **Vol. 10**, Issue 3, 406-421 (2010)
3. Norden B., Förster A., Balling N., Heat flow and lithospheric thermal regime in the northeast german basin, *Tectonophysics*, **Vol. 460**, Issue 1-4, 215-229 (2008)
4. Istok J.D., *Groundwater Modeling by the Finite Element Method*, American Geophysical Union, Washington (1989)
5. Javandel I., Doughty C., Tsang C.E., *Groundwater Transport: Handbook of Mathematical Models*, American Geophysical Union, Washington (1984)